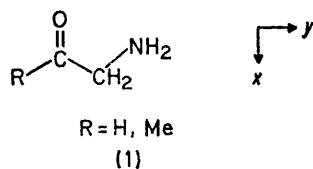


Orbital Interaction in Amino-ketones

By Charles C. Levin[†] and Roald Hoffmann,* Dept. of Chemistry, Cornell University, Ithaca, N.Y. 14850, U.S.A.
 Warren J. Hehre,[‡] Dept. of Chemistry, Carnegie-Mellon University, Pittsburgh, Pa.
 John Hudec, Dept. of Chemistry, The University, Southampton SO9 5NH

A study of the orbitals of α -aminoacetone and α -aminoacetaldehyde as a function of the two important torsions in these molecules is reported. The individual level shifts are much greater than the variation of the total energy. We identify four significant interactions affecting the level ordering. Each interaction has its distinctive conformational dependence. In order of decreasing spectroscopic importance the interactions are as follows. (1) Through bond coupling of the nitrogen and oxygen lone-pairs. (2) Through space interaction of these lone-pairs. (3) Hyperconjugation between the C-N σ^* level and the carbonyl π -system. (4) Direct overlap of the nitrogen lone-pair with the carbonyl π -system.

OUR continuing interest in the interaction of orbitals through space and through bonds prompted us to examine the electronic structure of a series of α -substituted carbonyl compounds (1). This particular



carbonyl grouping was examined for the following reasons. (1) Previous investigations¹ have focused on the interaction between equivalent lone-pairs; the series (1) serves as a useful prototype for the study of hetero-

nuclear non-bonded interaction, as well as lone-pair π -orbital mixing. (2) A substantial amount of experimental information has been obtained about the chemically important α -halogeno-analogues.² Further, some striking conformationally dependent spectroscopic anomalies have recently been noted for the coupled α -amino-chromophore.³ (3) A parallel interest in the electronic factors influencing optical rotatory strengths led naturally to an investigation of α -substituted carbonyl compounds.⁴ We present here calculations on α -amino-substituted acetaldehyde and acetone. Amino-compounds have been singled out for detailed examination because, in contrast to oxygen bearing substituents and halogen, the NH₂ group possesses only a single non-bonding electron-pair. This facilitates analysis of its interaction with the carbonyl group.

[†] Present address: Dept. of Chemistry, Smith College, Northampton, Mass. 01060.

[‡] Present address: Laboratoire de Chimie Théorique (490), Université de Paris-Sud, Centre d'Orsay, 91-Orsay, France.

¹ (a) R. Hoffmann, *Accounts Chem. Res.*, 1971, **4**, 1, and references cited therein; (b) R. Hoffmann, A. Imamura, and W. J. Hehre, *J. Amer. Chem. Soc.*, 1968, **90**, 1499; (c) J. R. Swenson and R. Hoffmann, *Helv. Chim. Acta*, 1970, **53**, 2331.

² (a) C. Djerassi, 'Optical Rotatory Dispersion,' McGraw-Hill Book Co., Inc., New York, 1960, chs. 9 and 10; (b) E. L. Eliel, N. L. Allinger, S. J. Angyal, and G. A. Morrison, 'Conformational Analysis,' John Wiley, New York, 1966, pp. 460-468.

³ (a) J. Hudec, *Chem. Comm.*, 1970, 829; (b) M. T. Hughes and J. Hudec, *ibid.*, p. 831.

⁴ C. Levin, unpublished data.

1973

A qualitative energy level diagram for a nonconjugated amino-carbonyl compound is shown in Figure 1.

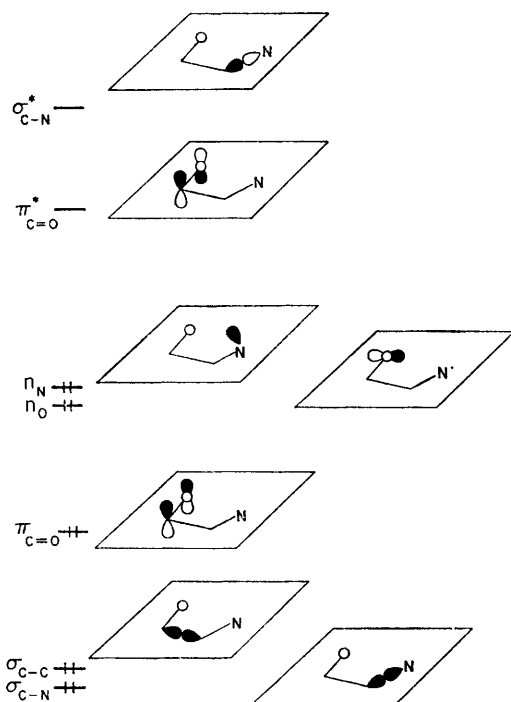


FIGURE 1 Qualitative energy-level diagram for the spectroscopically important molecular orbitals in a non-conjugated α -amino-carbonyl compound

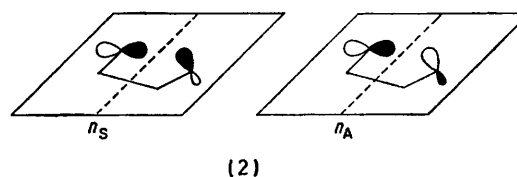
The construction starts from a localized basis of σ and σ^* levels, oxygen and nitrogen lone-pairs, and carbonyl π and π^* levels. We will rely on perturbation theory and molecular orbital calculations to inform us how this simple scheme, and in particular the positions of the spectroscopically important lone-pair, π , and π^* levels are to be modified.

In discussing the interaction of non-bonded electrons in an amino-ketone we will refer to those high-lying molecular orbitals which, while delocalized, can still be identified as carbonyl oxygen and amino-nitrogen lone-pairs, as n_O and n_N respectively. In the amino-ketones the highest occupied σ orbitals remain identifiable as some linear combination of these semilocalized lone-pairs. Moreover in- and out-of-phase combinations occur: $n_S = n_O + |\lambda|n_N$, $n_A = n_O - |\lambda'|n_N$, suggesting that the system 'remembers' its homonuclear antecedents, in which symmetry forced $\lambda = \lambda' = 1$. For this reason we classify the lone-pair combinations as (approximately) symmetric (n_S) or antisymmetric (n_A) with respect to the pseudo mirror plane or two-fold axis interchanging their positions. The convention is depicted in (2).

Five basic interactions will figure in setting the energy of the important orbitals—the two lone-pairs and the π and π^* orbitals of the carbonyl group.

⁵ See, *inter alia*, L. Salem, *J. Amer. Chem. Soc.*, 1968, **90**, 543; K. Muller, *Helv. Chim. Acta*, 1970, **53**, 1112.

(1) A through-space interaction of the oxygen and nitrogen lone-pairs which stabilizes the symmetric and destabilizes the antisymmetric combination of orbitals. It is well to recall here the familiar result that in calculations including overlap the antibonding combination



of two interacting orbitals is destabilized more than its bonding counterpart is stabilized.⁵ Through-space interaction depends on the overlap and thus on the proximity of the interacting orbitals.

(2) A through-bond coupling in which the symmetric lone-pair combination interacts with the lower lying C(1)-C(2) σ -bond orbital, which is also symmetric with respect to the pseudo mirror plane of (2). The levels repel one another and n_S moves to higher energy. In similar fashion n_A interacts with the antisymmetric σ^* orbital and goes to lower energy.¹ The energy separation between levels in this case is much larger since one of the orbitals is antibonding. Through-bond coupling, therefore, will effect n_S more than n_A . Interactions 1 and 2 are depicted schematically in Figure 2. The important conformational feature of through-bond coupling is that it requires the axes of the interacting orbitals to be respectively coparallel with the coupling σ bond.¹

(3) Hyperconjugation between the C-N bond and the carbonyl π -system. This interaction has been considered from a molecular orbital point of view by

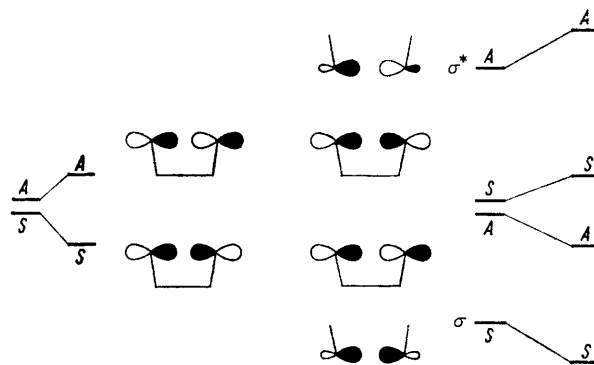


FIGURE 2 Through-space (left) and through-bond (right) interactions of lone-pairs. Symmetry classifications are with respect to a mirror plane or two-fold axis interchanging their positions

Allinger *et al.*⁶ who studied the red-shift induced in the cyclohexanone $n-\pi^*$ transition by axial halogen substituents. Their calculations indicated that interaction between the carbonyl π^* level and a relatively low lying C-X σ^* orbital, when the halogen is axial, gives rise to

⁶ N. L. Allinger, J. C. Tai, and M. A. Miller, *J. Amer. Chem. Soc.*, 1966, **88**, 4495.

the red-shift. Figure 3 is an interaction diagram summarizing Allinger's argument. Mixing of π^* with the higher lying σ^* C-X orbital in the axial epimer, but

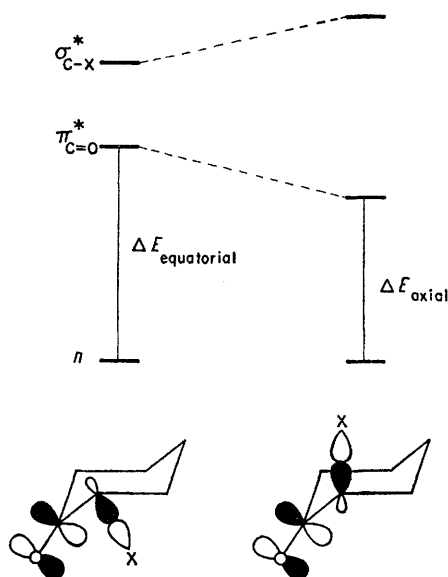


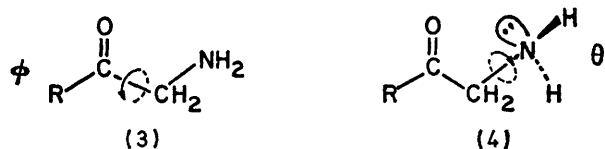
FIGURE 3 Qualitative interaction diagram depicting origin of the $n-\pi^*$ red-shift in axial α -halogenocyclohexanones

not in the equatorial one, moves it to lower energy, thus producing the observed red-shift. The strong conformational consequences of hyperconjugation have recently received renewed attention.⁷ Hyperconjugation is maximized when the C-N bond is aligned with the carbonyl π -system.

(4) Direct interaction of the nitrogen lone-pair with the carbonyl π -system. Clearly this is another type of direct through-space interaction, with an obvious conformational dependence.

(5) Hydrogen bonding between the carbonyl lone-pair and the amino-hydrogens.

Calculations.—Three degrees of freedom have been considered in the calculations. The first, a torsion described by the angle ϕ , corresponds to rotation about the C(1)-C(2) bond and is zero when the C(2)-N bond eclipses C(1)-O. The sense of rotation is indicated in (3). The second torsional degree of freedom is rotation

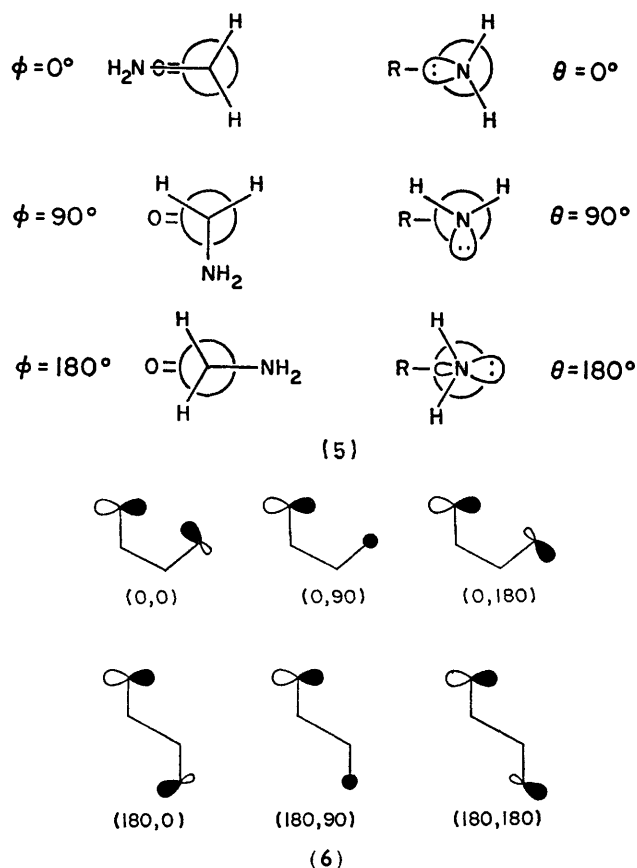


around the C(2)-N bond. This motion is described by the angle θ , taken to be zero when the nitrogen lone-pair eclipses C(1)-C(2) (independent of the value of ϕ). The

⁷ (a) T. G. Traylor, W. Hanstein, H. J. Berwin, N. A. Clinton, and R. S. Brown, *J. Amer. Chem. Soc.*, 1971, **93**, 5715; (b) R. D. Bach and P. A. Scherr, *ibid.*, 1972, **94**, 220; (c) R. Hoffmann, L. Radom, J. A. Pople, P. v. R. Schleyer, W. J. Hehre, and L. Salem, *ibid.*, p. 6221.

sense of θ is shown in (4). Structures (5) are Newman projections illustrating our definitions of θ and ϕ . The third degree of freedom is the C-C-N bond angle. We will consistently refer to amino-carbonyl conformations in terms of the angles ϕ and θ . For example, the conformation in which ϕ is 90° and θ 180° will be denoted (90,180); the value of ϕ will always come first. Our nomenclature for a number of important conformations is illustrated in (6). In cases where the C-C-N angle is varied its value will be indicated explicitly.

Calculations were performed at two levels of sophistication. (1) The semi-empirical extended Hückel (EH) method,⁸ which uses all valence electrons, includes overlap, but does not explicitly take electron repulsion into



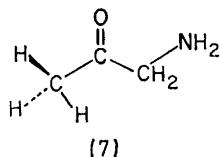
account. (2) STO-3G *ab initio* calculations⁹ in which each orbital of a minimal basis set of Slater-type orbitals is least-squares fitted by three Gaussian functions. The accurate *ab initio* calculations allow us to calibrate the less reliable EH results.

It should be noted that the EHT calculations were performed on α -aminoacetone, whereas the STO-3G

⁸ R. Hoffmann, *J. Chem. Phys.*, 1963, **39**, 1397; R. Hoffmann and W. N. Lipscomb, *ibid.*, 1962, **36**, 2179, 3489; *ibid.*, 1962, **37**, 2872.

⁹ (a) W. J. Hehre, R. F. Stewart, and J. A. Pople, *J. Chem. Phys.*, 1969, **51**, 2657; J. A. Pople, *Accounts Chem. Res.*, 1970, **3**, 317; (b) J. A. Pople and M. Gordon, *J. Amer. Chem. Soc.*, 1967, **89**, 4253.

computations used an aminoacetaldehyde model for obvious reasons of economy.* It will be shown that the interactions of interest are present in both compounds and we judge the errors in comparing the EH ketone with the STO-3G aldehyde to be minor. One place where a distinct difference should and does show up is in the $(180, \theta)$ conformations where the presence of the methyl group in aminoacetone is seen to destabilize this conformation relative to the same one in the aldehyde. All EH calculations on aminoacetone fix the methyl group in conformation (7).†



RESULTS

Figure 4a shows contours of the *ab initio* total energy as a function of θ and ϕ for α -aminoacetaldehyde. The

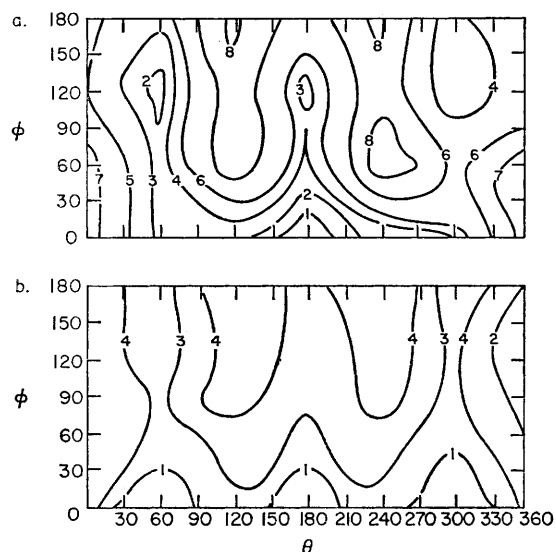


FIGURE 4 Total-energy contours for the two important torsions in the α -amino-carbonyl grouping. ϕ is the angle of rotation about the C-C bond, θ the angle of rotation about the C-N bond. Sense of rotations is defined in text. Numbers associated with contours are energies in units of 0.05 eV (1.15 kcal) above the global minimum in each diagram: a, STO-3G α -aminoacetaldehyde with energy zero at $(0,180)$. b, EH α -aminoacetone with energy zero at $(0,60)$

global minimum is at $(0,180)$, consistent with the expected staggering of the NH_2 group with respect to its

* STO-3G exponents are reported in ref. 9a; the aldehyde geometry employed is given in 9b. EH valence state ionization potentials were those of ref. 8. Slater exponents used were: H, 1.3; C, 1.625; N, 1.95; O, 2.275. A model aminoacetone geometry with 120° bond angles at the carbonyl carbon and all other angles tetrahedral was employed. Bond lengths were: C- CH_3 , 1.516; C- CH_2NH_2 , 1.500; C-N, 1.46; C-O, 1.23; C-H, 1.09; and N-H, 1.03.

vicinal RCH_2 , and in agreement with the experimentally observed preference of unsaturated functional groups in molecules such as acetone, acetaldehyde, and propylene

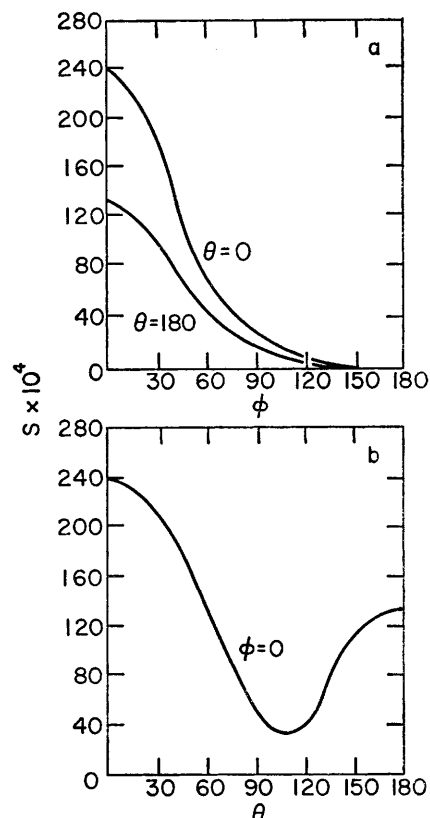


FIGURE 5 Overlap integral between oxygen p and nitrogen sp^3 lone-pairs in α -aminoacetone: (a) as a function of ϕ at θ values of 0° and 180° ; (b) as a function of θ at $\phi = 0^\circ$

to favour conformations in which one substituent on the α -carbon lies in the nodal plane of the π -system.¹⁰ For all values of $\phi > 30^\circ$ a sweep of θ at constant ϕ shows the minima at $\theta = 60, 180, 300$ that one expects of a dominant three-fold barrier. The EH surface for this molecule is in good qualitative agreement. In α -aminoacetone (Figure 4b) the general features of the aldehyde surface are retained, except for an obvious destabilization of the sterically encumbered region around $\phi = 180$.

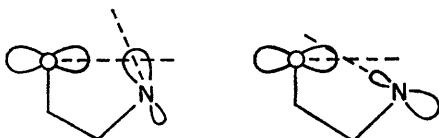
But the minor hills and valleys of the total energy mask much more pronounced variations of individual energy levels. These we now discuss, considering in turn each of the five basic interactions.

(1) *Through-space Interaction*. This interaction depends on direct overlap of the nitrogen and oxygen lone-

† The minimum energy conformation of acetone¹⁰ has one C-H bond of each methyl group eclipsing the C-O bond. We have used (7) instead to minimize the number of destabilizing C-H/N-H interactions in the $\phi > 90^\circ$ portion of the potential surface.

¹⁰ E. B. Wilson, jun., *Adv. Chem. Phys.*, 1959, 2, 367, and references therein.

pairs. That overlap is never large.† It reaches a maximum at (0,0) of 0.024 (with EH parameters), and falls off uniformly as ϕ is increased (Figure 5a). The θ variation, Figure 5b, is more interesting. Note that there is a reasonably large overlap at (0,180). The back lobe of the nitrogen lone-pair in the (0,180) orientation is considerably better disposed to overlap with the oxygen nonbonding electrons than the front lobe in the (0,0) conformation. Thus, despite the small amplitude of the back lobe at $\theta = 180^\circ$, its favourable orientation with respect to oxygen p_y gives rise to the substantial overlap observed.



Two slices of the ϕ, θ potential surface are particularly informative in analysing through-space interaction. Figure 6 depicts the behaviour of EH n_A and n_S as ϕ is varied at θ values of 0 and 180° . The analogous STO-3G results are plotted in Figure 7. We consider first the EH curves.

The n_A curve of Figure 6 is seen to have a shallow minimum at $\phi = 90^\circ$, and maxima at $\phi = 0$ and 180° , with the latter at lower energy. The energy lowering on

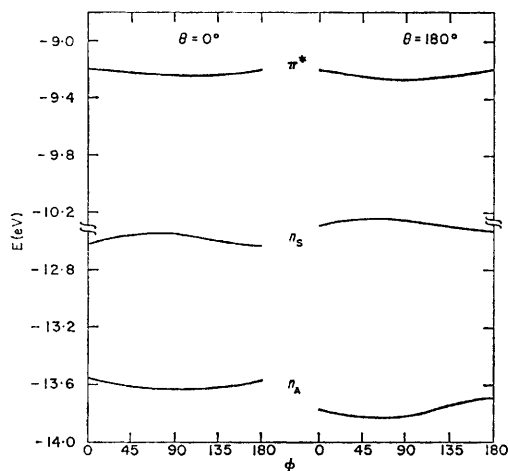


FIGURE 6 EH orbital energies for α -aminoacetone as a function of ϕ for θ values of 0 and 180°

going from $\phi = 0$ to $\phi = 90^\circ$ is clearly to have been expected from the accompanying decrease in de-

† Overlaps were evaluated between a Slater $2p_y$ orbital on oxygen and an sp^3 hybrid on nitrogen, at 30 degree intervals along the three degrees of freedom considered in Figure 5. Both EH and STO-3G geometries and exponents were used in the calculations; differences between pairs of overlaps calculated with the two sets of parameters were found to be negligible. Assuming sp^3 hybridization for the nitrogen lone-pair is, of course, an approximation. We judge it to be a reasonable one, however, since the overlap exhibits the same conformational dependence displayed in Figure 5 when either a pure p nitrogen lone-pair or an sp^2 hybrid replaces the present one.

stabilizing out-of-phase overlap. The subsequent increase in energy as ϕ varies from 90 to 180° cannot be explained in terms of through-space interaction and the other interaction mechanisms must be considered before

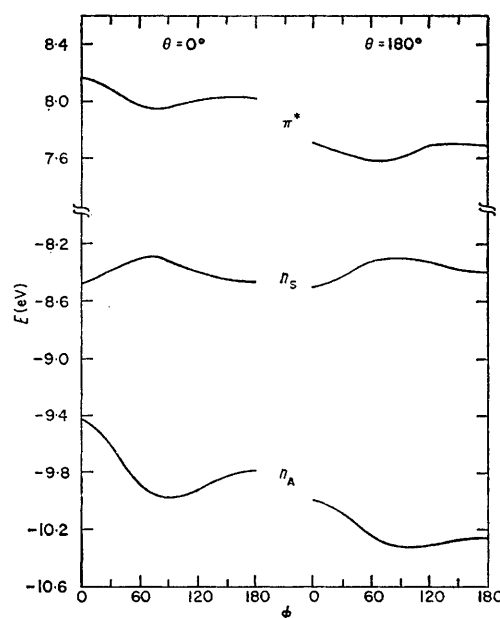


FIGURE 7 STO-3G orbital energies for α -aminoacetaldehyde as a function of ϕ for θ values of 0 and 180°

we try to rationalize this behaviour. The analogous n_A curve for $\theta = 180^\circ$ is decidedly more unsymmetrical, but its initial decrease in energy with increasing ϕ is again a consequence of decreasing lone-pair overlap. Note, however, that the $\theta = 180^\circ$ curve is lower in energy on the average by some 0.18 eV than its $\theta = 0^\circ$ counterpart. Returning to Figure 6 we see that the lower energy of the $\theta = 180^\circ$ curve is in part attributable to the smaller (hence less destabilizing) out-of-phase overlap. The two curves should approach one another on going to $\phi = 90^\circ$ and although this in fact does happen, the change is smaller than would have been anticipated from the ϕ dependence of the overlap.

The variation of the n_S levels with ϕ in Figure 6 clearly underscores the complementary behaviour of the lone-pair orbitals. The $\phi = 0$ and 180° points are now minima, the maximum in each case corresponds to the n_A minimum and this time the $\theta = 180^\circ$ slice is higher on the average by about 0.08 eV than the one at $\theta = 0^\circ$. Since n_S is the bonding combination of lone-pairs, the argument for n_A must be reversed; the orbital energy should then increase as ϕ goes to 90° .

The ϕ dependence of the STO-3G orbital energies for $\theta = 0$ and 180° is displayed in Figure 7. While the general qualitative resemblance to the corresponding extended Hückel curves is apparent, there are also some marked differences. Clearly the STO-3G energies exhibit a greater sensitivity to changes in ϕ than their EH analogues. The antisymmetric lone-pair curves are

seen to have the strongest ϕ dependence. As in the EH calculations the $\theta = 180^\circ$ slice lies substantially below the one at $\theta = 0^\circ$. In contrast the STO-3G n_S plots are nearly identical at $\theta = 0$ and 180° , a result which we would not have predicted from through-space considerations alone. Through-space interaction should, of course, push the (0,0) conformation to lower energy than (0,180).

(2) *Through-bond Coupling*.—When we allow our semi-localized lone-pair combinations to interact with other molecular orbitals of the same symmetry the most important mixings are found to be the C(1)–C(2) σ orbital with n_S and the corresponding σ^* orbital with n_A . From perturbation theory we know that any pairwise interaction leads to stabilization of the lower level and destabilization of the upper one. The amount of interaction will be proportional to the overlap of the levels and the reciprocal of their energy separation.^{1,5} As a result, n_S is pushed up in energy to a greater extent than n_A is pushed down. This indirect interaction of lone-pairs *via* other orbitals has been termed through-bond coupling.¹ Its principal consequence in the case at hand is to overcome through-space interaction and push n_S above n_A .

Again we focus on the lone-pair levels as through-bond coupling is probed in our amino-carbonyl prototypes. The $\phi = 0$ and $\phi = 180^\circ$ slices shown in Figures 8 and 9 illustrate the θ dependence of n_S and n_A ,

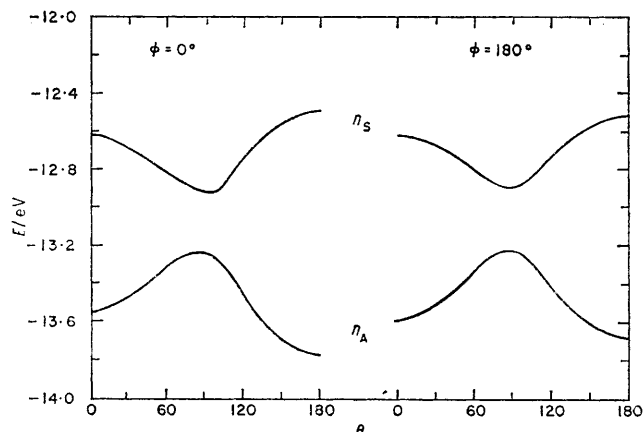


FIGURE 8 EH orbital energies for α -aminoacetone as a function of θ for ϕ values of 0 and 180° ; π^* is insensitive to variation of θ

and provide the most information about through-bond interaction. The EH curves in Figure 8 exhibit a marked θ dependence. Both n_A levels have minima at $\theta = 0$ and $\theta = 180^\circ$, and a maximum at $\theta = 90^\circ$. The corresponding n_S slices are seen to behave in a complementary way. Since through-bond coupling results from interaction of the σ and σ^* levels of C(1)–C(2) with the adjacent lone-pairs, it should be a maximum when the overlap between them is greatest. Clearly the orientations of maximum overlap occur at $\theta = 0$ and $\theta = 180^\circ$; accordingly, n_A should be maximally lowered, n_S maximally raised, and this is just what we see.

The corresponding $\phi = 0$ and $\phi = 180^\circ$ slices of the STO-3G surface are plotted in Figure 9. The resemblance between the curves calculated by the two methods is

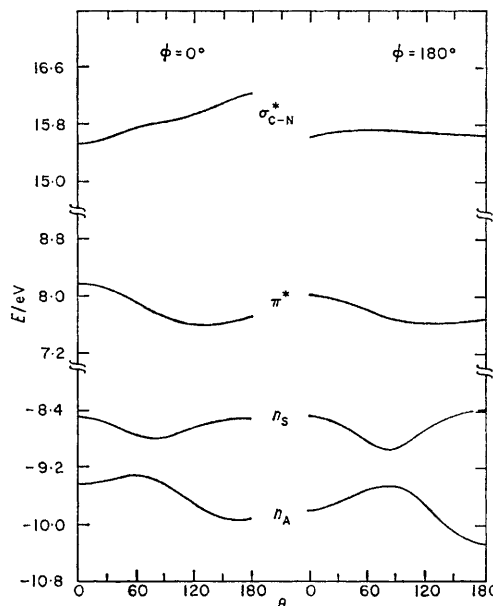
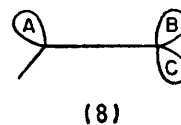


FIGURE 9 STO-3G orbital energies for α -aminoacetaldehyde as a function of θ for ϕ values of 0 and 180°

indeed quite close. The complementary nature of the n_S and n_A curves is apparent again in the STO-3G results.

There are several interesting features of the constant ϕ slices in Figures 8 and 9. First we note that the n_S – n_A splitting is greater at $\theta = 180^\circ$ than at $\theta = 0^\circ$. A rationalization for this in the $\phi = 0^\circ$ case is that through-space interaction is larger at (0,0) than at (0,180); as the overlap is decreased from $\theta = 0$ to $\theta = 180^\circ$ n_S will go up in energy, n_A will go down, and the splitting will increase. No such argument, however, can be used for the $\phi = 180^\circ$ case where through-space overlap is non-existent. Strikingly, the differential splitting here is nearly the same as in the $\phi = 0^\circ$ case.

The large splitting at $\theta = 180^\circ$ could be explained if through-bond coupling were greater than at 0° . In our initial study of through-bond coupling,^{1b} it was demonstrated that the vicinal overlap between *trans* sp^2 hybrids A and C in (8) is greater than between the *cis* hybrids A and B.



The magnitude of through-bond coupling is largely controlled by overlaps of this kind so that for carbon sp^2 hybrids the interaction is larger at $\theta = 180^\circ$. An analogous calculation for sp^3 hybrids on C and N, however, actually shows the overlap in question to be slightly smaller at 180° than at 0° .

A second puzzling feature perhaps related to the first is the high sensitivity of n_A to variations in θ . As we have noted, the effects of through-bond coupling should be much more pronounced in n_S than in n_A , since the latter is far removed from σ^* in energy.

We can obtain additional information about through-bond and through-space interactions by examining the lone-pair level behaviour as the C-C-N angle is varied. This is done for the STO-3G results in Figure 10. The n_S curves for tetrahedral C-C-N lie above those for n_A as we have noted previously. The n_A curve for the (0,0) conformer lies some 0.35 eV above that for (180,0) at tetrahedral C-C-N suggesting that the through-space lone-pair repulsion significantly outweighs their interaction through bonds. This level moves up sharply with decreasing C-C-N. Concomitantly, the through-space stabilized n_S counterpart drops in energy, but not nearly as rapidly. Again through-space interaction prevails. The difference in slopes reflects the greater through-bond coupling in the symmetric combination

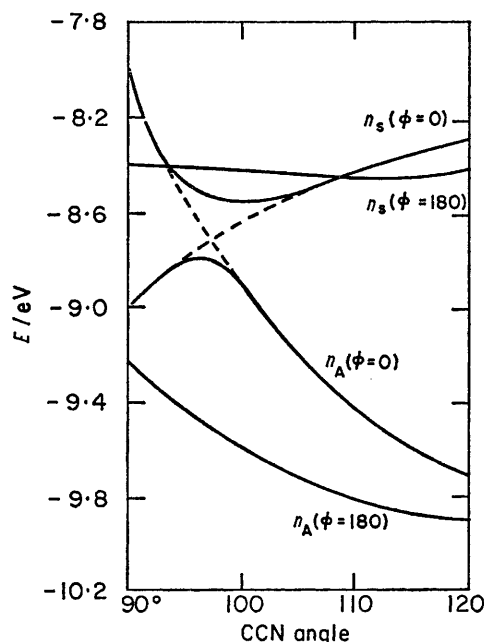


FIGURE 10 STO-3G lone-pair energies for α -aminoacetaldehyde as the CCN angle is varied from 120 to 90°. There is an avoided level crossing (dashed lines) at CCN \approx 97°

than in the antisymmetric one. As anticipated, the destabilizing through-bond component attenuates the downward movement of n_S at (0,0) to a greater extent than does the analogous stabilizing component in n_A . An avoided level crossing of the (0,0) non-bonded combinations is seen to take place at a C-C-N angle of ca. 97°.

It is well to review here the symmetry assignments we have made for the non-bonding levels. By classifying them symmetric or antisymmetric with respect to a pseudo mirror plane interchanging lone-pair positions, we have formally restricted their interaction to other

levels of the same pseudo-symmetry. Strictly speaking, n_S , n_A , σ , and σ^* all have the same symmetry. In the (0,0), (0,180), (180,0), and (180,180) conformations, where a true mirror plane exists, these levels are all symmetric with respect to it. The remaining conformations possess only trivial symmetry and all molecular orbitals will interact. The extent of interaction, of course, still depends on the usual overlap and reciprocal energy factors alluded to earlier. In designating orbitals as pseudo-symmetric or antisymmetric, however, we have implicitly recognized that overlap between levels of opposite pseudo symmetry is very nearly zero and so too their interaction.

The avoided level crossing in Figure 10 is a consequence of the low symmetry of the aminoacetaldehyde. Both lone-pair combinations are symmetric with respect to the mirror plane containing the four heavy atoms. The non-crossing rule guarantees that levels of the same symmetry will never cross, their mutual interaction forcing them to repel one another. Nevertheless, if the interaction between levels is small, as it is here, the intended crossing is only narrowly avoided as we see in Figure 10. The intention of the n_A level to cross n_S at (0,0) is clearly manifest in the wave-functions, where the highest filled level at C-C-N = 90° is the antisymmetric combination of lone-pairs.

No avoided level crossing is observed for the (180,0) curves. The energy of n_A increases with decreasing C-C-N, but not nearly so rapidly as for the (0,0) orientation. This was also the case in the EH calculations and inspection of the wave-functions again confirms that the destabilization results from an antibonding interaction between the aldehydic hydrogen and nitrogen lone-pair. The symmetric combination is essentially invariant to the C-C-N variation, exhibiting a slight minimum around 105°. The invariance of n_S at (180,0) is surprising since the anticipated increase in through-bond interaction should give it a marked upward slope. Indeed, the presence of this destabilizing component was used to explain why n_S went down less rapidly than n_A went up in the (0,0) conformation.

A clue to the solution of this puzzle is again found in the wave-functions. In contrast to the n_A orbital, the interaction between the aldehydic hydrogen and nitrogen lone-pair electrons is a bonding one. Why then is the bonding combination of this pair found in a higher-energy orbital than the corresponding antibonding one? The explanation is clearly the same as that for the appearance of n_S above n_A . In the absence of through-bond coupling the symmetric lone-pair level will lie below the antisymmetric combination. This time it is the symmetric combination of aldehydic hydrogen and nitrogen lone-pair which does so. Through-bond coupling then pushes n_S above n_A .

(3) *Interaction of the C-N Orbitals with the π System.*— While this interaction does not directly involve the lone-pair electrons, it influences the spectroscopic properties of amino-carbonyl compounds and is therefore considered here. As noted previously, Allinger *et al.*⁶

found that the σ^* C-X orbital of an axially disposed halogen induces the red-shift of the $n-\pi^*$ transition in α -halogenocyclohexanones by depressing the π^* level of the carbonyl group. To examine this interaction, we follow the one electron π^* energy as a function of ϕ .

The extended Hückel calculations already presented in Figure 6 show a π^* minimum at $\phi = 90^\circ$ for both the $\theta = 0$ and $\theta = 180^\circ$ slices. These minima are quite shallow, lying only 0.04 and 0.06 eV, respectively, below the $\phi = 0^\circ$ values. An axial substituent in an idealized cyclohexanone corresponds to $\phi = 120^\circ$, and π^* energies here differ only slightly from the energies of the maxima. It is interesting to note in passing that the ϕ dependence of n_s is somewhat greater than that for π^* at both values of θ . The EH curves thus indicate that the $n-\pi^*$ red shift in amino-carbonyl compounds is a composite of two effects: a lowering of π^* together with a raising of n_s . Depending upon the particular value of ϕ , the n_s contribution may be the larger one. At $\phi = 120^\circ$, for example, the n_s component dominates in our calculations.

Inspection of the extended Hückel π^* wave-functions confirms Allinger's original observations. The anti-bonding σ^* C-N orbital mixes into the lower lying π^* in a bonding way when the amino-group is at or near $\phi = 90^\circ$. This mixing was depicted in Figure 3 for the (90,0) conformer.

The STO-3G π^* energy slices in Figure 7 show qualitatively the same ϕ dependence as their EH analogues. For the $\theta = 0$ and $\theta = 180^\circ$ energy slices, π^* minima are at $\phi = 80$ and 65° respectively. The energy drop from $\phi = 0^\circ$ in each case is larger than for EH, being about 0.16 eV for $\theta = 0^\circ$ and 0.12 eV for $\theta = 180^\circ$. The n_s levels are seen to have maxima at about the same ϕ values. At the idealized axial ϕ value of 120° the π^* red-shift component is slightly larger in the $\theta = 0^\circ$ conformer but smaller at $\theta = 180^\circ$.

In assessing the relative contributions of n_s and π^* contributions to the red-shift, it is helpful to consider the slice of the ϕ, θ surface for which ϕ is fixed at 90° and θ is varied from 0 to 330° . The STO-3G curves are shown in Figure 11. The high sensitivity of n_s to variations in θ witnessed in other constant ϕ slices is also evident here. The π^* energy variation is small in comparison to n_s . The calculations imply that the $n-\pi^*$ transition in amino-carbonyl compounds is extremely sensitive to the angle of rotation about the C-N bond.

Caution must be exercised in applying these results to the prediction of spectral properties. We have approximated the θ, ϕ dependence of the $n-\pi^*$ excited state by the behaviour of the one-electron energy differences. The correct expression for the singlet excitation energy is of course

$$\Delta E_{ij} = \epsilon_j - \epsilon_i - J_{ij} + 2K_{ij}$$

Coulomb and exchange integrals would have to be evaluated. Moreover, there is ample evidence that a single-configuration description of the excited state is

H

inadequate. While a more sophisticated treatment is necessary before our results are viewed with confidence, we feel that the primary features obtained from an examination of one-electron energy gaps will be retained for the following reasons. (1) We are dealing with small geometry perturbations within one molecule and on a related sequence of transitions. (2) In an important recent study of $n-\pi^*$ transitions,¹¹ it was found

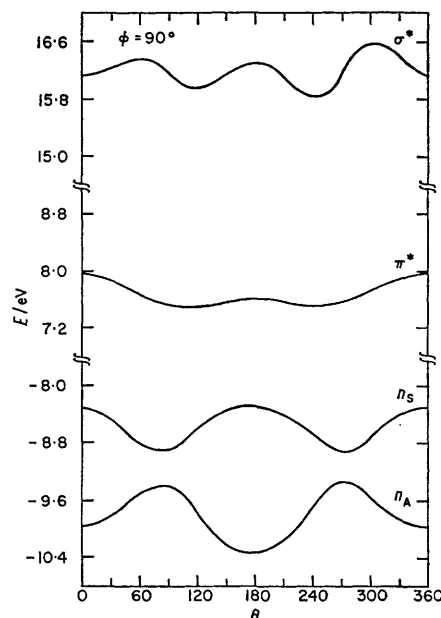


FIGURE 11 STO-3G orbital energies for a α -aminoacetaldehyde as a function of θ at $\phi = 90^\circ$

that within a related series of molecules, the variation of $\epsilon_i - \epsilon_j$ was greater than that of the two-electron part of the transition energy.

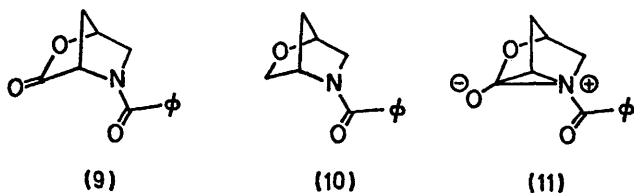
Remaining Interactions.—Interactions (4) and (5) are covered more briefly as they turn out to be less important than the preceding ones. Mixing of the nitrogen lone-pair with the π system should be most important for conformations in the neighbourhood of (90,0) and (90,180), where overlap between the two groups is strongest. One indication that this mixing is small comes from a comparison of the $\phi = 0$ and $\phi = 180^\circ$ lone-pair energy-slices with the one at $\phi = 90^\circ$. Allowing for the fact that loss of lone-pair through-space overlap in the $\phi = 90^\circ$ conformation increases the n_s-n_A splitting, there is little difference between the curves. Removal of through-space interaction between the nitrogen lone-pair and π system by increasing θ to 90° would cause a significant change in the nonbonded levels, if this interaction were an important one. The attendant change in energy for this motion is, in fact, substantial but is present to the same extent when the amino-group lies in the plane of the carbonyl system.

Further evidence that the nitrogen π -system interaction is relatively small derives from inspection of the

¹¹ R. Ditchfield, J. E. DelBene, and J. A. Pople, *J. Amer. Chem. Soc.*, 1972, **94**, 703.

n_B wave-functions at $\phi = 90^\circ$. Only a small admixture of the carbonyl π -system is observed. In contrast, the θ dependence of the STO-3G π^* energy at $\phi = 90^\circ$ (see Figure 11) hints at such a mixing. Interaction of π^* with the nitrogen nonbonded electrons should be maximum at θ values of 0 and 180° . Upward displacement of π^* would be greatest at these points, and this is what is observed in Figure 11.

An instance where interaction between the nitrogen lone-pair and the π system may be significant is in (9). Recent measurements of the amide rotational barrier show it to be smaller by 2 kcal mol⁻¹ than in (10).¹² The



authors postulate the transannular interaction indicated in (11). Inspection of models indicates that the non-bonded electrons and carbonyl group are canted directly toward one another. The rigid bicyclic framework allows no deviation from this orientation.

Hydrogen bonding was probed by inspection of overlap populations between the amino-hydrogen and carbonyl oxygen for conformations in which these atoms closely approach one another. Our previous experience¹³ suggests that for hydrogen bonding to be important the overlap populations must be 0.05 or larger. The computed values fall an order of magnitude short, and so we think the hydrogen bond effect is unimportant.

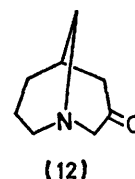
DISCUSSION

The electronic descriptions of the α -amino-carbonyl chromophore emerging from the two sets of calculations are in reasonable qualitative agreement. In each case the two highest filled orbitals are lone-pair combinations with the symmetric one at higher energy. The lone-pair splitting is a sensitive function of through-space and through-bond interactions with the latter predominating. Splitting varies from 0.3 to 1.3 eV in EH and from 0.4 to 2.0 eV in the STO-3G calculations. Through-space interaction is most important in the (0,0) and (0,180) conformations, falls off rapidly as the amino-group departs from a *cis*-coplanar orientation, and has a maximum magnitude of *ca.* 0.2–0.3 eV. Through-bond coupling is a maximum in the (ϕ ,0) and (ϕ ,180) conformers, where vicinal overlap between the lone-pairs and component orbitals of the adjacent σ bond is greatest.

Effects of lone-pair interactions will be most evident in the spectral properties of amino-carbonyl compounds. Unsubstituted ketones normally exhibit $n-\pi^*$ absorption near 290 nm. α -Amino-ketones absorb at 300–335 nm,

depending on the individual compound. One of us^{3a} has analysed the spectra of a number of α - and β -amino-ketones from an empirical point of view. The red-shift in α -amino-ketones has been attributed to two factors: (1) Coupling of π and π^* with the C–N σ and σ^* orbitals when the two groups are nearly parallel, *i.e.* for an axial amino-substituent. This is the Allinger argument⁶ considered earlier. (2) Interaction between the carbonyl π system and an axial nitrogen lone-pair when the latter is *trans* diaxial to the C(1)–C(2) bond. It is also found that in cases where the *trans* diaxial condition of (2) is fulfilled a second transition at much shorter wavelength and higher intensity (ϵ *ca.* 500) is observed.

The u.v. spectrum of 1-azabicyclo[3,3,1]nonan-3-one, (12), has recently been reported.^{3b} This interesting α -amino-ketone is geometrically quite constrained, inspection of models indicating that its most likely conformation is one with ϕ between 150° and 180° and θ also close to 180° . The long-wavelength transition in (12) is red-shifted with decreasing solvent polarity, as expected for an $n-\pi^*$ transition. In hexane λ_{\max} is



found at 330 nm. The red-shift (relative to 290 nm) thus corresponds to 0.52 eV. If we use the $\theta = 90^\circ$ level positions to simulate the absence of through-bond coupling in our calculations then a comparison of the position of the n_B level at $\theta = 90^\circ$ with that at $\theta = 180^\circ$ (Figures 8 and 9) yields a calculated red-shift of the same magnitude.

From the point of view of the calculations, the second, 235 nm, transition of (12) should originate from the penultimate n_A level. Several aspects of the observed spectrum^{3b} support this contention. First, decreasing solvent-polarity shifts the absorption to longer wavelength just as in the case of the longer wavelength transition. Further, the high-energy transition disappears when the nitrogen is protonated. Finally, the 95 nm (1.52 eV) difference in λ_{\max} between the two absorptions^{3b} is in good qualitative agreement with the lone-pair splitting for a conformation approaching (180,180).

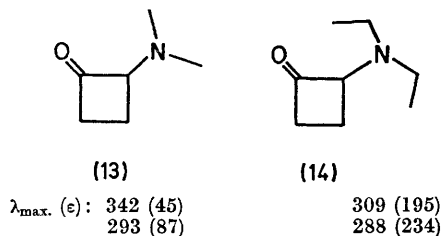
One question which immediately arises in connection with this assignment for the low-wavelength transition is why it is not observed at other θ values. Since the n_A energy is a minimum at $\theta = 180^\circ$ its energy will increase at intermediate angles, thereby red-shifting the second transition into a region where it should be readily detectable. Indeed this may well be the case. Consider, for example, the dialkylaminocyclobutanones (13)

¹² P. S. Portoghese and J. G. Turcotte, *Nature*, 1971, **230**, 457.

¹³ W. Adam, A. Grimison, R. Hoffmann, and C. Zuazaga deOrtiz, *J. Amer. Chem. Soc.*, 1968, **90**, 1509.

1973

and (14), each of which exhibits two distinct bands.^{14†} It would be of interest to see if both transitions are red-shifted in less-polar solvents. Another revealing feature



of the amino-ketones (13) and (14) is the rather large change in the long wavelength absorption on going from dimethyl to diethyl substitution. The bulkier ethyl groups undoubtedly alter the conformation of the amino-group with respect to the carbonyl. It would be unrealistic to attempt assigning conformations to the homologues with the limited information available, but the point clearly emerges that the spectral properties are quite sensitive to the degree of freedom we have called θ .

Additional hints of through-bond interaction and its strong θ dependence can be gleaned from o.r.d. data for the optically active steroidal ketone in Table I. Columns

TABLE I

O.r.d. data for 17 β -amino-17 α -pregn-5-en-2-ones^a

X	λ_1^b	$[\alpha_1]^c$	λ_2^b	$[\alpha_2]^c$
NH ₂	331	-90 (max.)	297	-841
NHMe	336	+375	294	-1385
NMe ₂	342	+2125	286	-3340

^a D. F. Morrow, M. E. Butler, and E. C. Y. Huang, *J. Org. Chem.*, 1965, **30**, 582. ^b Wavelength (in nm) of first (long wavelength) and second (short wavelength) extrema. ^c Amplitude (in degrees) of first and second extrema.

2 and 4 refer to positions of the long and short wavelength Cotton curve extrema; columns 3 and 5 give the signed amplitudes of these extrema. The sign of the Cotton effect changes as methyl groups replace amino-hydrogens and amplitudes increase markedly especially at the short wavelength side. The highly unsymmetrical appearance of the curves may indicate a second absorption of opposite sign on the short wavelength side of the first.

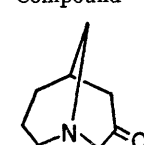
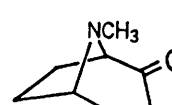
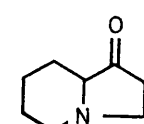
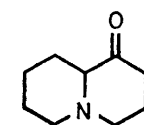
Rotatory strengths of the $n_S-\pi^*$ transition calculated with extended Hückel wave-functions exhibit the same high sensitivity to θ as observed for the one-electron

† If these are $n-\pi^*$ transitions we should compensate for the high solvent polarity by adding 10–20 nm to each $\lambda_{\max.}$ before making comparisons with other compounds or the calculations.

orbital energies.⁴ Significantly, small variations in θ can alter both the sign and magnitude of the rotatory strengths. Also relevant is the fact that the $n_A-\pi^*$ rotatory strength always had the opposite sign to that for the $n_S-\pi^*$ transition. It has been noted,^{3a} in fact, that the low wavelength transition, when observed, always has a rotatory strength sign opposite to that at longer wavelength. The difference in signs would not be surprising in view of the opposite pseudo symmetries of the lone-pair combinations.

Table 2 presents additional spectral data for α -amino-ketones with rigid bicyclic frameworks. θ and ϕ Values

TABLE 2

Spectral data for some α -amino-ketones with fixed conformations					
Compound ^a	ϕ^b	θ^b	$\lambda_{\max.} (\epsilon)^c$	Solvent	Ref.
	160	165	330 (55)	Hexane	<i>f</i>
	180	330	314 (68) ^d	Ethanol ^d	<i>g</i>
	150	300	314 (48)	Iso-octane	<i>h</i>
	170	270	293 (29)	Iso-octane	<i>h</i>

^a Compounds listed in approximate order of increasing deviation from coplanarity of n_O and n_N . ^b Estimated from models. ^c $\lambda_{\max.}$ in nm; ϵ = molar extinction coefficient. ^d To compare with other compounds, one must allow for a 10–20 nm red-shift on going to less-polar solvents. ^e Progression of bands. ^f Reference 3b. ^g S. Archer and R. M. Bell, *J. Amer. Chem. Soc.*, 1960, **82**, 4642. ^h S. Yamada and T. Kunieda, *Chem. Pharm. Bull. (Japan)*, 1967, **15**, 490.

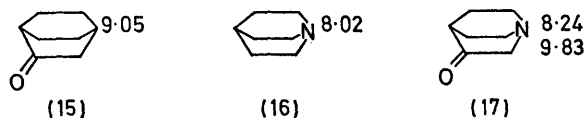
in columns 2 and 3 have been estimated from models. Compounds are listed in order of increasing deviation of the nitrogen lone-pair from coplanarity with its counterpart on oxygen. The close correlation between magnitude of through-bond coupling and size of the red-shift is evident once again.

A final experimental manifestation of through-bond lone-pair interaction is found in photoelectron data¹⁵ for the series (15)–(17). Numbers to the right of the

¹⁴ J. M. Conia and J. L. Ripoll, *Bull. Soc. chim. France*, 1963, 755.

¹⁵ J. M. Mellor and J. Hudec, unpublished data.

structures are first ionization potentials in electron volts. The second ionization potential for amino-ketone (17) is



also included. The 1.03 eV splitting between isolated lone-pairs in (15) and (16) increases to 1.59 eV in (17) with the onset of through-bond coupling. While a

differential splitting of 0.56 eV is of the magnitude we calculate, the larger ionization potential in (17) relative to (16) would not have been anticipated.

We are grateful to the National Institutes of Health (GM 13468) and the National Science Foundation for support of our research.

We have benefited from helpful comments and criticisms by R. B. Davidson during the preparation of the manuscript.

[2/1934 Received, 14th August, 1972]